catalysts

MDPI

Article

Comparison of Direct and Mediated Electron Transfer for Bilirubin Oxidase from Myrothecium Verrucaria. Effects of Inhibitors and Temperature on the Oxygen Reduction Reaction

Riccarda Antiochia [1], Diego Oyarzun [2], Julio Sánchez [3] and Federico Tasca [3,*]

1 Department of Chemistry and Drug Technologies, Sapienza University of Rome, 00185 Rome, Italy; riccarda.antiochia@uniroma1.it
2 Departamento de Química, Universidad Tecnológica Metropolitana, Av. José Pedro Alessandri 1242, Santiago 7750000, Chile; diequim@gmail.com
3 Facultad de Química y Biología, Universidad de Santiago de Chile, Santiago 9170020, Chile; julio.sanchez@usach.cl
* Correspondence: Federico.tasca@usach.cl

Received: 11 October 2019; Accepted: 28 November 2019; Published: 11 December 2019

Abstract: One of the processes most studied in bioenergetic systems in recent years is the oxygen reduction reaction (ORR). An important challenge in bioelectrochemistry is to achieve this reaction under physiological conditions. In this study, we used bilirubin oxidase (BOD) from *Myrothecium verrucaria*, a subclass of multicopper oxidases (MCOs), to catalyse the ORR to water via four electrons in physiological conditions. The active site of BOD, the T2/T3 cluster, contains three Cu atoms classified as T2, T3α, and T3β depending on their spectroscopic characteristics. A fourth Cu atom; the T1 cluster acts as a relay of electrons to the T2/T3 cluster. Graphite electrodes were modified with BOD and the direct electron transfer (DET) to the enzyme, and the mediated electron transfer (MET) using an osmium polymer (OsP) as a redox mediator, were compared. As a result, an alternative resting (AR) form was observed in the catalytic cycle of BOD. In the absence and presence of the redox mediator, the AR direct reduction occurs through the trinuclear site (TNC) via T1, specifically activated at low potentials in which T2 and T3α of the TNC are reduced and T3β is oxidized. A comparative study between the DET and MET was conducted at various pH and temperatures, considering the influence of inhibitors like H_2O_2, F^-, and Cl^-. In the presence of H_2O_2 and F^-, these bind to the TNC in a non-competitive reversible inhibition of O_2. Instead; Cl^- acts as a competitive inhibitor for the electron donor substrate and binds to the T1 site.

Keywords: oxygen reduction reaction; bilirubin oxidase; direct electron transfer; mediated electron transfer; osmium polymer

1. Introduction

One of the most interesting phenomena to have been intensively studied over the last 25 years is the electronic coupling between the redox cofactor of proteins and electrodes by direct (DET) or mediated electron transfer (MET) reactions [1,2]. The oxygen reduction reaction (ORR) is considered one of the most important electrocatalytic reactions due to its implication in biological systems as well as in industrial processes [3,4]. Multicellular living organisms use oxygen as an electron (e−) acceptor, for example, in the respiratory chain [5,6]. In fuel cells chemical energy is converted into electrical energy through the ORR [3,4,7–9]. Many fungi and bacteria use oxygen as a signalling molecule [10–12] to form hydrogen peroxide and degrade wood and lignocelluloses. In nature this reaction is catalysed

mainly by Cu containing proteins, such as multicopper oxidases (MCO) [13,14]. MCOs constitute a family of enzymes that includes laccase (Lc), ascorbate oxidase, bilirubin oxidase (BOD), CotA, Fet3p, CueO and ceruloplasmin [15]. They are important for Fe metabolism and related disease states, antibiotic biosynthesis, biotechnology, bioremediation, biosensing and BFCs [8,15]. These enzymes can be immobilized directly on the electrode (DET) or using small redox molecules (MET) that facilitate electron transfer between the redox centre of the enzyme and the electrode [1,2,6,16]. Several studies have been conducted on Cu enzymes to gather more information about the ORR and how to reproduce this reaction with synthetic and biological materials. In this sense, MCOs have been identified as particularly efficient catalysts of the ORR, carrying out fast, four-electron reduction at low overpotentials [17]. BODs, a sub-class of MCOs containing four Cu ions per one enzyme molecule, were discovered in 1981 by Tanaka and Murao [18], and first used for the detection of bilirubin [19] and later for the reduction of O_2 [20,21]. According to their magnetic and optical properties, the Cu atoms are classified into three types T1, T2 and a binuclear T3 (T2 and T3 sites are combined in a tri-nuclear cluster or TNC) [16,22–24]. The single-electron oxidation of substrates occurs at the proximal T1 site, with the 4-electron reduction of O_2 taking place at the TNC [19]. The 4 electrons are quickly transferred from the T1 site to the MCO TNC via a histidine-cysteine-histidine ligand [19]. In 2008 the resting oxidised form of the enzyme was proposed and lately an AR form was characterized by crystallography, spectroscopy and electrochemistry [25,26]. AR was found to occur only with high potential MCO where the T1 has a high enough potential to perform the one-electron oxidation of the TNC that produces AR [27]. The activation for catalysis of these different forms was assessed. The results showed that the AR form can only be activated by low-potential reduction, in contrast to the resting oxidized form, which was activated via T1 at high potential [26]. This difference in activity was correlated to differences in redox states of the two forms [26].

A main limitation for enzyme-modified electrodes is related to the electron transfer between the enzyme active sites and solid conducting supports (electrodes). Alternatively, mediated electron transfer (MET) involves small redox molecules that shuttle electrons from enzyme to electrode [5,28]. Most of the highest reported current densities are produced by MET-type electrodes, because enzyme molecules may be electrochemically active in multiple layers and at any orientation [29]. Osmium polymers have been used extensively as electron-transfer mediators to bind MCOs to the electrode surface [30–39]. Nevertheless, the reactivation of BOD in the presence of osmium polymer has never been studied before. Herein, the electron transfer processes for the different states of BOD in the presence of an osmium polymer were studied and compared to DET.

It is known that the activity of Lc and BOD can be inhibited by halide anions; however, BOD is less sensitive to Cl^- ions than Lc [23,40]. For example, F^- acts as a non-competitive inhibitor that interrupts electron transfer between MCOs' T1 and TNC [23,41]. Other studies on Lc with H_2O_2 have demonstrated a reversible non-competitive inhibition of the enzyme due to oxidation of the T3 Cu site [31]. To the best of our knowledge, the effect of inhibitors was never studied in the presence of redox mediators and compared to DET. In this work the effect of pH, temperature and of the inhibitors was studied when in the presence or in the absence of osmium polymer and the action from H_2O_2 and F^- anions were analysed in the activation of the AR form in the DET and MET of bilirubin oxidase on graphite electrodes.

2. Results and Discussion

2.1. Electrochemical Characterization

MCOs couple the oxidation of bilirubin to the reduction of oxygen to water through four copper atoms: a T1 Cu atom that functions as an electron relay and a trinuclear cluster (2T3 denominated as T3α, T3β and 1T2 Cu atoms) where the reduction occurs. The substrate for T1 can be substituted with a source of electrons, for example, a graphite electrode.

Therefore, when BOD is immobilized on the surface of graphite electrodes the T1 redox centre is responsible for shuttling the electrons from the electron surface to the T2/T3 cluster.

The cyclic voltammograms provide important information about the immobilized enzyme. It is important to note that electrocatalysis by adsorbed enzymes presents a residual slope and therefore voltammetry curves show a linear response, suggesting that the electrode follows Ohm's law. However, Armstrong and co-workers explain that this effect could be because the enzymes are not adsorbed homogeneously on the electrode [42,43]. At the same time, this effect is much more evident when the studies were carried out at different pH and temperature as will be described below. Meanwhile, spectroscopies and electrochemistry are used to identify different resting forms of MCOs. One of these forms corresponds to a fully oxidized resting form (RO), which is derived from the decay of the native intermediate (NI) [27]. Another resting state called alternative resting form (AR) was identified in some high redox potential MCOs, such as BOD from CotA, *Bacillus subtilis* [44], *Myrothecium verrucaria* [45] (Mv-BOD), *Trachyderma tsunodae* [45] (Tt-BOD), *Magnaporthae orizae* [45] (Mo-BOD), *Pleurotos* ostreatus and *Bacillus pumilus* [45] (Bp-BOD). Figure 1A shows typical cyclic voltammograms (CVs) of an edge graphite electrode modified with 10 µL of 0.2 mM BOD solution in the absence and in the presence of O_2. The scans were carried out cathodically in 0.1 M phosphate buffer solution at pH 7. In the absence of O_2 (blue line), non-faradaic processes were observed due to the large surface area of the graphite electrode and its corresponding charging/discharging process. A non-modified graphite electrode would present an almost identical cyclic voltammogram, and therefore it is not shown in the figure. The black and red lines in Figure 1A correspond to the first and second scans, respectively, in O_2 saturated buffer for a fresh electrode. For the first scan (Figure 1A, black line) the voltammogram on the forward sweep is characterized by two hysteresis observed at ~0.40 V and ~0.1 V vs SCE, indicating an activation step at low potentials for the ORR. During the second scan the onset for O_2 reduction occurs at ~0.5 V. The hysteresis obtained during the first scan suggests that many molecules of the enzyme in direct electron contact with the graphite electrode are not catalytically active in a redox state corresponding to the AR form of the enzyme [27,46,47]. Therefore, the AR form can be activated for O_2 catalysis, at low potential for the Cu sites that form the TNC. In the purification process of BOD from *Myrothecium verrucaria* it is common to use NaCl [48], which could cause the formation of the AR. These results are in agreement with Poulpiquet and co-workers, as they show that an activation step at low potentials for O_2 reduction corresponds to the partially reduced AR form in which TNC T2 and T3α are reduced and T3β is oxidized [47]. Furthermore, the same group recently demonstrated that the full reduction of the AR form of Lc cannot occur via T1, but only via T3β [47]. A DET process through the TNC supposes that the TNC is sufficiently close to the interface to exchange electrons. The insert of Figure 1A shows a magnification of the potential zone of 0.4 V to observe the hysteresis of the first scan for BOD activation. In the second cycle (red line) the onset for the ORR occurs at ~0.5 V potential without presenting any hysteresis, indicating the activation of the enzyme. The osmium redox polymers allow an efficient electron transfer by wiring multiple layers of the immobilized molecules and promoting stable adsorption [30]. A high redox potential OsP ($E^{0\prime}$~0.21 V vs. SCE) was selected from a previously reported library of Os polymers [49]. Figure 1B depicts the electrochemical response of a freshly prepared BOD-OsP modified graphite electrode in 0.1 M phosphate buffer solution, at pH 7.0 in the absence and in the presence of O_2, and at a scan rate of 5 mVs^{-1} the scans swept from 0.8 V to −0.2 V. In the absence of O_2 (black line), the characteristic redox wave of the OsP with an $E^{0\prime}$ ~0.21 V for Os^{III}/Os^{II} redox couple is clearly defined. In the presence of O_2 (red line first scan, blue line second scan) the first scan of the voltammogram shows two hysteresis at ~0.32 V and ~ −0.05 V, suggesting again that the T2/T3 centre for the ORR is activated at low potentials, while during the second scan the onset for O_2 reduction is seen at 0.40 V. When the potential values of the hysteresis under DET and MET are compared (from Figure 1A,B), a displacement of ~40 mV may be seen in the cathodic direction for T1 and T2/T3. Most probably this displacement is caused by the reduction of the OsP, which should be followed by the reduction of the Cu atoms. The ligands of the OsP could affect the BOD sites to make the ORR take place or the AR form could be activated only at sufficiently low potentials for O_2

reduction. Similar current densities and onsets for the ORR of the BOD-OsP electrodes have been obtained before [33], but this is the first time that activation of BOD enzyme has been reported in the presence of the OsP hydrogel. The activation of the T2/T3 redox centre could be the result of the reduction of the centre by the T1 cluster or directly by the electrode or by electrons that flow from OsP redox sites. Solomon and co-workers [27] showed that when T3 are partially oxidized and T2 is fully oxidized (AR form of the enzyme), the T2/T3 sites have a significantly lower electron-affinity than the high potential T1 Cu. The fact that the T2/T3 reduction occurs at lower potentials in the presence of the OsP could indicate that the reaction occurs principally through the OsP atoms, and therefore reducing the Os atoms is necessary before the electrons are transferred to the T2/T3 couple [27].

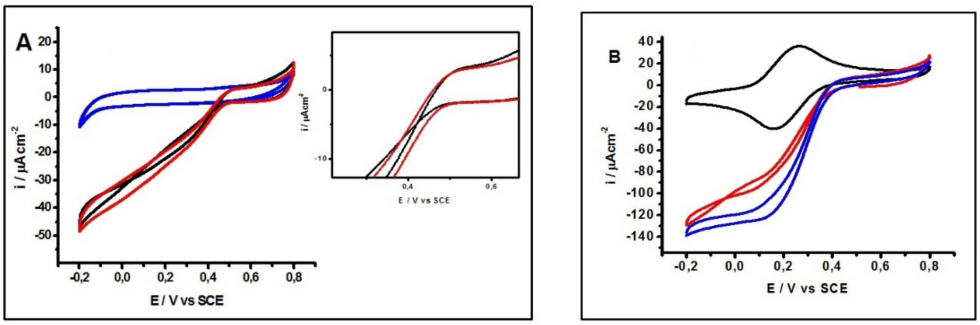

Figure 1. (**A**) Cyclic voltammogram of a BOD modified electrode. Insert: zoom on the 0.4 V to observe the activation zone of the second cycle (black line). (**B**) Cyclic voltammogram of the Os/Poly/BOD/ modified electrode. Conditions: 0.1 M phosphate buffer solution, pH 7.0 in absence (blue line) and in presence (black line first scan, red line second scan) of O_2. Scan rate: 5 mV s^{-1}.

2.2. *Effect of pH*

In solution, *mv*BOD is active in a wide pH range from pH 5 to pH 8 [45,50,51]. Also it has been proven that *mv*BOD is very stable in the presence and in the absence of Os polymer or other mediator, losing around 10% of activity during one day under operating conditions [45,50–52]. The effect of pH on the MCO catalytic mechanism has only been partly elucidated, but it is well resumed in [45,53]. Figure 2A shows cyclic voltammograms using a BOD modified electrode in phosphate buffer 0.1 M in the presence of O_2 at different pH (pH 8 black line, pH 7 red line, pH 6 green line, and pH 5 blue line). Phosphate buffer was used to obtain various pHs because it is known that it does not cause interference with the catalytic activity of the enzyme. The capacity of the buffer in the aforementioned range is of 0.02 moles and therefore it can be used for the purpose. The shape of the curves is the same for pH 5, 6 and 7 in the first scan, where two hystereses can be observed at different potential values that, in all cases shift to more negative potentials as the pH is increased. Hysteresis is consistent with the presence of the AR form of the enzyme on the surface of the electrode and with the low-potential half wave that corresponds to the T2/T3 reduction, indicating a proton dependent reaction [27,46,47]. The reduction of the T2/T3 sites follows ~60 mV dependence per pH units. During the second scan (after reduction of the T2/T3 cluster) the low-potential half wave disappears. The high potential wave corresponds to the T1 site and does not change from the first to the second scan but it follows ~30 mV dependence per pH unit. At pH 8, to observe the hysteresis at low potential half wave is very difficult and during the second scan very low activity could be measured. This is in agreement with the studies of dos Santos [42], which indicates that at this pH the enzyme is not active. In acidic conditions the intramolecular processes are fast: the current rate is determined by the T1 redox cycling but the T1 potential does not define the catalytic activity. At neutral or alkaline pH, the intramolecular processes are slow and determine the current rate as well as the T1 potential defines the catalytic activity. Furthermore, the current decreases at alkaline pH due to the lack of proton transfer and electrochemical driving force as suggested by do Santos and co-workers [42]. For the second scan, the onset for the ORR depends on pH, moving to more positive potentials as the pH decreases. Figure 2B shows the voltammograms corresponding

to an electrode modified with osmium polymer, in phosphate buffer 0.1 M in the presence of O_2 at different pH (pH 8 black line, pH 7 red line, pH 6 green line, and pH 5 blue line). Table 1 summarizes the potential of the high and low potential hysteresis for oxygen reduction in DET and MET, at pH 7. The first scan is characterized by two hysteresis at different potential values at pH 5. In this case, as the pH increases the potential values displace to more negative potentials. However, at pH 6 and 7 the low wave potential is not clearly defined, probably because the ET from the OsP to the TNC is so fast that this process is not observed. The hysteresis at low wave potential is consistent with the presence of an AR form of the enzyme after reductive activation below this hysteresis; this AR form is converted into the RO form of the enzyme confirmed through the second cycle of the voltammogram. At pH 8 hysteresis is not observed and only the wave for the Os^{III}/Os^{II} redox couple is clearly defined with E′ ~0.27 V. The first and the second scan yielded the same results in practice, evidencing the inactivation of the enzyme at this pH. It is important to note that the current density for hysteresis at low potential half wave increases when the OsP is present compared to the DET, because the ET is favoured from the enzyme to the electrode by the Os atoms present in high concentration. Likewise, hysteresis at the low potential half wave for MET shifts to negative values due to the OsP redox potential (the redox mediator should be in the reduced form to donate electrons to the cluster) improving the ET from the electrode to OsP and from OsP to the T2/T3 cluster. It is noteworthy that under physiological conditions, these four electrons are exchanged sequentially through the T1 copper site of the enzyme and further transferred by internal electron transfer (ET) to the trinuclear T2/T3 cluster.

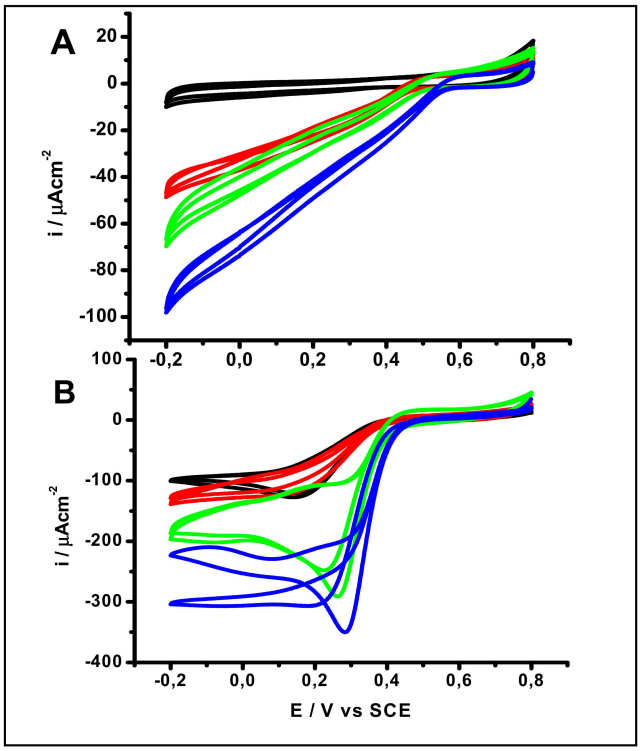

Figure 2. Cyclic voltammetry of (**A**) BOD and (**B**) Os/Poly/BOD/PEGDGE at various pHs. Conditions: phosphate buffer 0.1 M, at various pHs: pH 8 (black), pH 7 (red), pH 6 (green), pH 5 (blue) Scan rate: 5 mV s^{-1}.

Table 1. Summary of the potential corresponding to the high potential and low potential hystereses for oxygen reduction in DET and MET, at pH 7.

	DET		MET	
pH	High Potential Hysteresis, V	Low Potential Hysteresis, V	High Potential Hysteresis, V	Low Potential Hysteresis, V
7	0.440 ± 5	0.100 ± 5	0.300 ± 5	0.000 ± 5

2.3. Temperature Effect

The oxygen reduction catalysis is affected by various factors, among which is temperature [38]. *mv*BOD in solution is fully active from 30 °C to 60 °C whereas it loses 50% of original activity at 20 °C [6]. The effect of the temperature on the catalytic activity of BOD in DET and MET systems in the ORR was studied. Figure 3A shows cyclic voltammograms for O_2 reduction at different temperatures, all at 5 mV s^{-1} using a BOD electrode in phosphate buffer 0.1 M and in presence of O_2. The studies were performed in a temperature range from 10 °C to 50 °C. Figure 3A shows cyclic voltammograms in the presence of O_2 at 10 °C (black line) and 50 °C (green line). During the first scan, at both temperatures hysteresis close to 0.4 V and 0.35 V, respectively, were observed, suggesting the presence of the AR form. At 50 °C the activity is 10% lower than at 30 °C. Figure 3B shows similar experiments to Figure 3A but in the presence of OsP. At 10 °C (black line) and at 20 °C (results not shown), hysteresis appears near 0.30 V during the first scan for BOD activation. At 30 °C (red line) and 50 °C (green line) a different behaviour is seen. Not clear hysteresis can be observed and differences between the catalytic current and the shape of the voltammograms (~10% of catalytic current) of the first and second scan are minor. Probably due to the swelling of the polymer, the electron transfer at these temperatures is so fast that the enzyme is activated very fast and is ready for oxygen reduction. It should be noted that at 50 °C the enzyme presents a higher activity than at 10 °C, which is in contrast with the results showed in Figure 3A, where no major difference appears at different temperatures. These results can be explained due to a faster interaction between the enzymatic redox sites and the OsP.

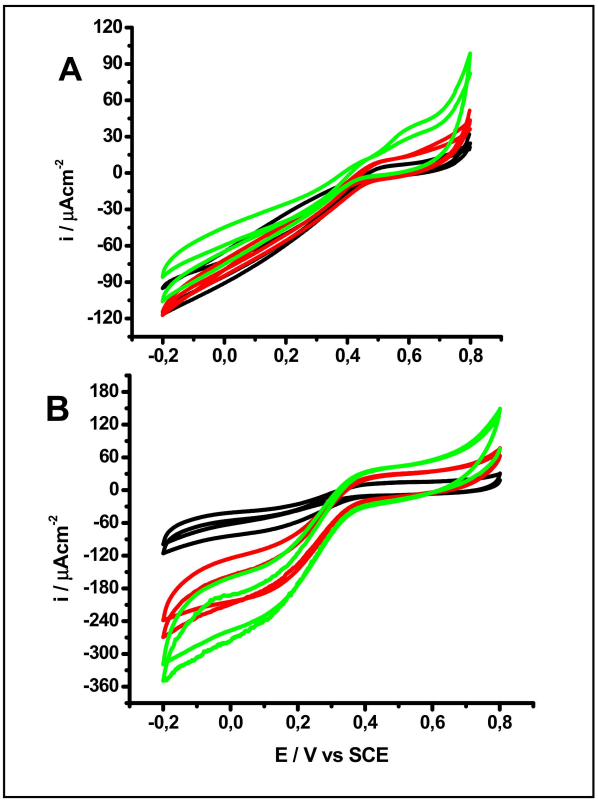

Figure 3. Cyclic voltammetry of (**A**) BOD and (**B**) Os/Poly/BOD/PEGDGE at various temperatures. Conditions: phosphate buffer 0.1 M, pH 7, at different temperature: 10 °C (black), 30 °C (red), 50 °C (green). Scan rate: 5 mV s^{-1}.

2.4. Inhibitory Effect

In 2010, Calvo et al. [31] reported the first evidence of the inhibitor effect of H_2O_2 on MCOs. Milton and Minteer have reported the reversible inhibition of Lc by H_2O_2 under DET and MET with ABTS (2,2-azino bis(3-ethylbenzothiazoline-6-sulfonic acid) [23,54].

Figure 4A shows chronoamperometry measurements of an activated BOD modified electrode polarized at E = 0 V in the presence of O_2 and during the additions of 1 μM, 5 μM and 10 μM H_2O_2. Clearly, the presence of 1 μM of H_2O_2 negatively affects the electrocatalytic current and the subsequent additions of H_2O_2 (5 μM and 10 μM final concentrations) confirm the inhibitory process. Figure 4B shows cyclic voltammetric measurements of the same electrode employed during the chronoamperometry of Figure 4A in the absence of H_2O_2. The second scan (black line) clearly shows that an activation process takes place after the first scan (reductive process, red line) but hysteresis is not evident, as opposed to the previous voltammograms. The current density obtained after reduction was ~−41 μAcm^{-2}. Therefore, 71% of the activity was recovered. Figure 4B shows the effect of H_2O_2 on a BOD-OsP under the same conditions shown in Figure 4A. After the first addition of 1 μM H_2O_2 no change in the current density was observed. However, when H_2O_2 was added at final concentrations of 10 μM, a small decrease of current density was seen (~8% compared to the constant current of the chronoamperometry). Therefore, only high concentrations (<10 μM) of H_2O_2 can inhibit the electrocatalytic process in the presence of OSP. In order to reactivate the process the system needs to be saturated with O_2, so it can displace the peroxide located in the cluster. The voltammogram corresponding to the enzyme activation is illustrated in Figure 4D. In this case the current density reaches −239 μAcm^{-2} at 0 V. Therefore, when compared with the constant current of chronoamperometry measurements, it represents 80% of the recovery in enzyme activity. In both cases the results for DET and MET indicated that the enzyme showed a non-competitive reversible inhibition of O_2 by exogenous H_2O_2, which interacted with the TNC [31,32]. Under DET and using a BDO cathode, Milton and co-workers [23] suggested that H_2O_2 follows a non-competitive inhibition. These same authors reported the inhibition of laccase with H_2O_2 under both conditions: DET and MET with 2,2′-azino-bis(3-ethylbenzothiazoline-6-sulfonic acid) (ABTS) as redox mediator. They indicated that laccase under DET follows an uncompetitive inhibition by H_2O_2 binding to the T2/T3 cluster [54]. Calvo showed the inhibition of laccase by H_2O_2 using an multilayer osmium derivative poly (allylamine) redox mediator and found that exogenous H_2O_2 inhibits laccase due to T3 Cu^{+1} [31].

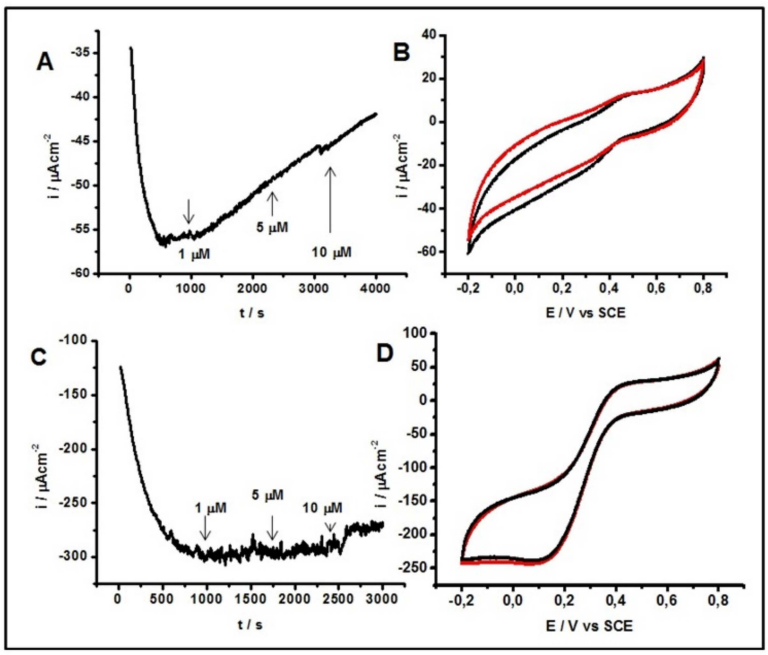

Figure 4. Chronoamperometry of (**A**) BOD and (**C**) Os/Poly/BOD/PEGDGE. Conditions: phosphate buffer 0.1 M, pH 7, at E = 0 V (vs SCE) in presence of O_2 and with H_2O_2 addition at different concentrations 1 μM, 5 μM and 10 μM. Later to the H_2O_2 addition the cyclic voltammetry of (**B**) BOD and (**D**) Os/Poly/BOD/PEGDGE was recorded. Scan rate: 5 mV s^{-1}.

BODs can be inhibited by halide anions such as F^- and Cl^- [23]. Figure 5A shows the chronoamperometric of a BOD electrode in the presence of O_2 at pH 7 at various NaF concentrations (1 μM, 5 μM and 10 μM). In DET experiments concentrations up to 10 mM were added where a considerable current density loss was observed for the ORR. Figure 5B shows cyclic voltammetric measurements in the absence of F^- of the same electrode used in Figure 5A. Once more, the reactivation process is not very clear and there are not many differences between the first and second scan, indicating that the enzyme keeps its activated form and the inhibition process is not caused by the oxidization/reduction process to the TNC, because O_2 is not able to completely displace the fluoride ions from the active site. In Figure 5C chronoamperometric measurements are shown in the presence of an OsP at different NaF concentrations (100 μM, 1000 μM and 10000 μM). In this case only very high concentrations of NaF (>1 mM) would affect the electrocatalytic process. These results indicate that fluoride acts as a non-competitive inhibitor, binding to the T2/T3 cluster of the enzyme, interrupting the ET between T1 and the TNC, and finally preventing the ORR. EPR studies revealed that F^- interacts with TNC only in the presence of the oxidized T3 Cu (II) [55]. This would explain why a bigger inhibition in the redox mediator electrode is observed, since F^- is blocking the active site favoured by the OsP. Figure 5D shows cyclic voltammetry of the BOD reactivation at pH 7 without inhibitor, where it is possible to displace F^-, recovering 95% of the activity. These results are in agreement with those published by other authors, which suggest that F^- ions inhibit DET and MET [55–57].

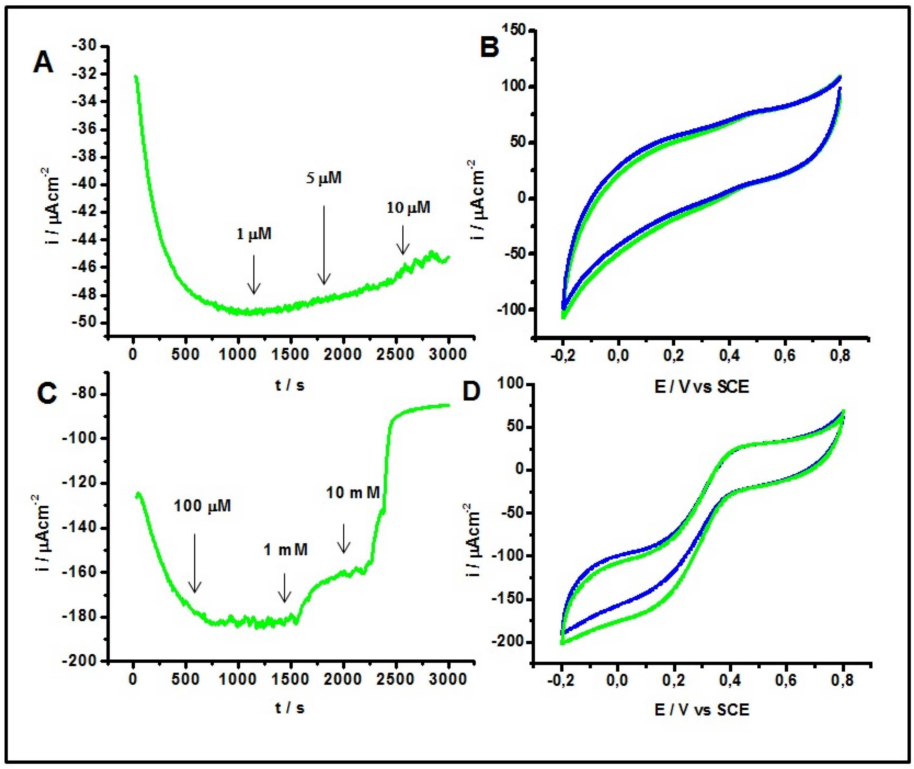

Figure 5. Chronoamperometry of (**A**) BOD and (**C**) Os/Poly/BOD/PEGDGE. Conditions: phosphate buffer 0.1 M, pH 7, at E= 0 V (vs SCE) in presence of O_2 and with NaF addition. The concentrations of NaF added were 1 μM, 5 μM and 10 μM for the BOD and 100 μM, 1000 μM and 10,000 μM for the Os/Poly/BOD/PEGDGE electrode, respectively. Later to the NaF addition the cyclic voltammetry of (**B**) BOD and (**D**) Os/Poly/BOD/PEGDGE was recorded. Scan rate: 5 mV s^{-1}.

Another halide that inhibits the BOD is Cl^-. Figure 6A shows the chronoamperometric measurements for a BOD modified electrode in the presence of O_2 at different NaCl concentrations (1 mM, 0.01 M and 0.1 M). This figure evidences a decrease in the current density when Cl^- concentration >0.1 M is added. Figure 6B shows the cyclic voltammetry in a fresh solution in the absence of Cl^- and in

the presence of O_2 using the same electrode used for the chronoamperometry shown in Figure 6A. When the BOD is reactivated O_2 displaces the Cl^- located in the T1 site because no activation in the second cycle (brown line) can be observed. Figure 6C shows the effect of Cl^- on a BOD electrode modified with an OsP under the same conditions indicated above, in which a slight decrease in the current (4%) can be appreciated when the maximum concentration of Cl^- (0.1 M) is added. The voltammograms in the absence of Cl^- (using the same electrode in Figure 6C) are shown in Figure 6D. This figure shows catalytic activity that suggests that Cl^- act as a competitive inhibitor with respect to the electron donor substrate, and that O_2 displaces the Cl^- present in the T1 site. These results indicate that the enzyme can show a reversible inhibition behaviour led by chloride ions so Cl^- blocks the ET to the T1 site, instead of binding it to the TNC [58]. However, Jensen and co-workers [59] have witnessed the Cl^- inhibition effect on laccase in DET. Nevertheless, high resistance to Cl^- inhibition under DET has been reported in nanostructured electrodes, which suggests that they avoid Cl^- entry to the T1 site [56,57].

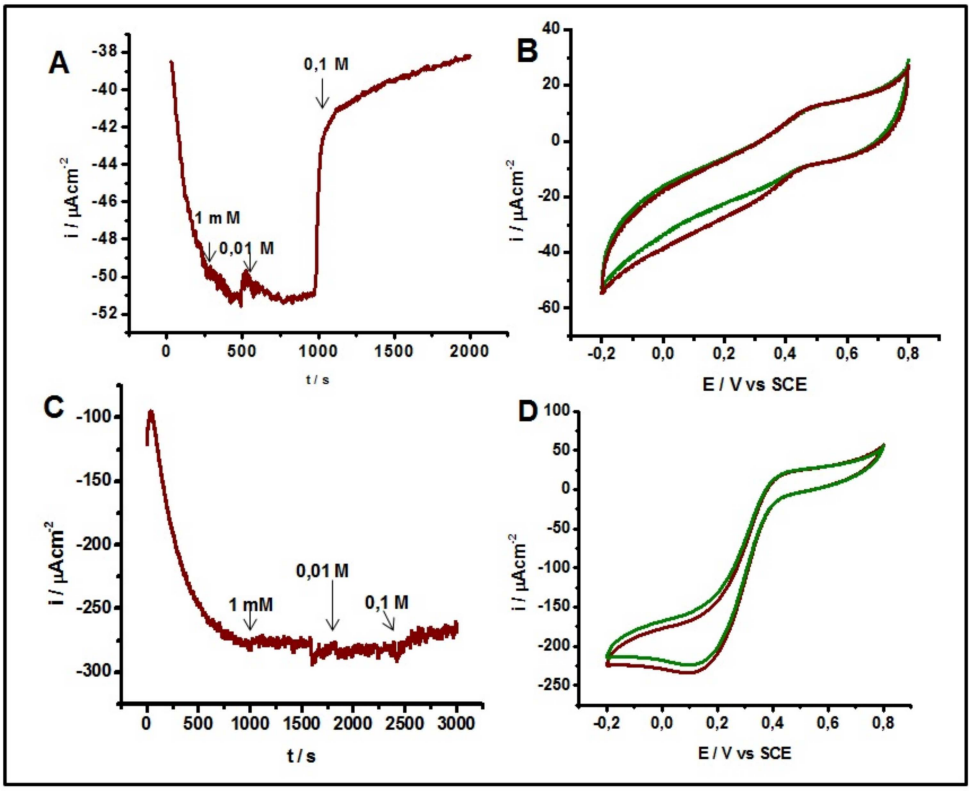

Figure 6. Chronoamperometry of (**A**) BOD and (**C**) Os/Poly/BOD/PEGDGE. Conditions: phosphate buffer 0.1 M, pH 7, at E = 0 V (vs SCE) in presence of O_2 with NaCl addition at different concentrations 1000 µM, 10,000 µM and 100,000 µM. Cyclic voltammetry of (**B**) BOD and (**D**) Os/Poly/BOD/PEGDGE was recorded after the NaCl addition. Scan rate: 5 mV s^{-1}.

3. Experimental

3.1. Chemicals

K_2HPO_4, KH_2PO_4, 30% H_2O_2, NaF, NaCl and Poly (ethylene glycol) diglycidyl ether (PEGDGE), 2,2′-Azino-bis(3-ethylbenzothiazoline-6-sulfonic acid) (ABTS) and dithionite were purchased from Sigma Aldrich (San Luis, MO, USA) with ACS purity grade. High purity (90% or higher concentration of pure enzyme) *Myrothecium verrucaria* BOD "Amano 3" was donated by Amano Enzyme Inc., (Madeline, LN, USA). The received lyophilized powder was stored at −20 °C and 0.2 mM enzyme solution were fresh prepared. The activity of the enzyme solution was checked by monitoring ABTS oxidation at 420 nm (ε = 36 $mM^{-1}cm^{-1}$) over time with stirring in 0.1 M sodium phosphate buffer. The activity test was performed on each prepared batch and resulted to be 12 ± 2 U/mg whereas one unit

is defined as the amount of enzyme that oxidizes 1 μmol of ABTS per minute. The Osmium polymer $[Os(bpy)_2(PVI)_{10}Cl]^{2+/+}$ was synthetized at the National University of Ireland, Galway following procedures already reported in [60–63]. The average molecular weight of the polymer as determined by viscometry in ethanol was 130,000 g/mol [64]. By taking the mean value of the anodic and cathodic peak potentials of the CV, the E°-value of the Os polymer was found to be +180 mV vs. SCE (sat. KCl). The polymer is positively charged so to increases the solubility in water and the electrostatic interaction with anionic regions of the enzyme [64].

3.2. Preparation of BOD and BOD-OsP Modified Electrodes

Edge-plane pyrolytic graphite electrodes of 5 mm diameter were purchased from PINE (Durham, NC, USA). To prepare the electrodes, the end of a rod was wet polished with an in-house made electrode polisher and waterproof 800 and 1200 grit emery sandpaper and then sonicated in deionized water for 10 min to remove any residual impurities. This process also insures a highly reproducible real surface area with less than 10% deviation in the charging/discharging current of blank electrodes measured during cyclic voltammetry experiments [65,66]. The electrodes were then rinsed with Milli-Q water and air-dried. Later, 10 μL of enzyme solution (~0.2 mM) were placed on top of the polished rod and adsorption was allowed to occur. The electrodes were then stored overnight at 4 °C under controlled humidity. After 24 h electrodes were rinsed with Milli-Q water and after being inserted in a Teflon holder, they were ready to use as working electrodes. For the MET experiments, electrodes were modified through the same previous treatment (mechanical cleaning) and drop adsorption, depositing first 10 μL of the OsP dissolved in water (10 mg/mL) [49,60]. This solution was mixed with 20 μL of a BOD 0.2 mM solution and 5 μL of PEGDGE 10 mg/mL. The electrodes were kept overnight at 4 °C under controlled humidity for complete cross-linking.

3.3. Electrochemical Measurements

The electrochemical measurements were carried out in a conventional three-electrode cell. The electrodes used were a platinum spiral wire as counter electrode and a saturated calomel electrode as reference electrode. All the results are related to this reference electrode. Current densities were calculated based on the geometrical area of the working electrode. The experiments were conducted with at least three repetitions. A 0.1 M phosphate buffer (K_2HPO_4, KH_2PO_4) was used as electrolytic solution. The range of pH effect was studied between 5 to 8. The inhibitors used were H_2O_2, NaF and NaCl added at different concentrations. Electrochemical experiments were performed with an AUTOLAB PGSTAT204 potensiostat (Utrecht, Netherlands).

4. Conclusions

In this study, MvBOD was studied in the absence and in the presence of OsP. The influence of pH and temperature, as well as the effects of H_2O_2, Cl^-, and F^- inhibitors were evaluated. Particular attention was paid to the activation process of the enzyme and therefore to the reduction of the AR form. The ORR can be activated only if the potential of the enzyme is reduced at values lower than 0.1 V, where TNC's T2 and T3α are reduced and T3β is oxidized. In the presence of the OsP a shift of ~40 mV in the cathodic direction for the T1 and for the T2/T3 reduction can be observed probably because the OsP needs to be reduced before the electrons can be transferred to the Cu sites. The ORR process was studied at various pHs. Both DET and MET showed very low activity at pH 8. Under DET the T2/T3 reduction showed a proton dependent reaction [27,46,47] that follows ~ 60 mV dependence per pH units. Instead, T1 reduction follows ~ 30 mV dependence per pH unit. Under MET the T1 reduction process still follows ~ 30 mV dependence per pH unit, while the reduction of the trinuclear cluster at pH 5 and 6 cannot be determined. At 30 °C and higher temperatures, in the presence of OsP, hysteresis, which enhances the activation of the enzyme, was not evident. In both DET and MET, in the presence of H_2O_2, a non-competitive reversible inhibition occurred, suggesting that it binds to the TNC of the enzyme. In MET, the inhibition occurs only at very high concentrations (>10 μM of H_2O_2).

The inhibition by halides showed a different mechanism for F^- and Cl^-. F^- acts as a non-competitive inhibitor, binding to the oxidized T3 Cu (II) [55]. In the case of F^-, under DET, small concentrations inhibited the ORR, while during MET concentrations higher than 1 mM this was necessary. After using a fresh buffer solution no hysteresis were observed. Cl^- showed a competitive inhibition [56,57]. Nevertheless, the inhibition process occurred only during DET and at very high concentrations of NaCl (>0.1 M). Using fresh buffer, a small reactivation process took place, which indicates that Cl^- could cause the AR form of the enzyme. During MET the inhibition process was less evident, suggesting that the presence of the OsP prevents the interaction between Cl^- and the T1 site.

Author Contributions: Data curation, J.S.; Formal analysis, R.A.; Investigation, D.O.; Writing—original draft, F.T.

Funding: This research was funded by Fondecyt Project 1181840.

Acknowledgments: F.T. thanks for financial support the Fondecyt Project 1181840, and Proyecto Basale Dicyt.

Conflicts of Interest: The authors declare no conflict of interest.

References

1. Balzani, V. (Ed.) *Electron. Transfer in Chemistry*; WILEY-VCH Verlag GmbH & Co. KGaA: Weinheim, Germany, 2001.
2. Gray, H.B.; Winkler, J.R. *Electron. Transfer in Metalloproteins*; Wiley-VCH: Weinheim, Germany, 2001.
3. Gamella, M.; Koushanpour, A.; Katz, E. Biofuel cells—Activation of micro- and macro-electronic devices. *Bioelectrochemistry* **2018**, *119*, 33–42. [CrossRef] [PubMed]
4. Solomon, E.I.; Stahl, S.S. Introduction: Oxygen Reduction and Activation in Catalysis. *Chem. Rev.* **2018**, *118*, 2299–2301. [CrossRef] [PubMed]
5. Gewirth, A.A.; Thorum, M.S. Electroreduction of Dioxygen for Fuel-Cell Applications: Materials and Challenges. *Inorg. Chem.* **2010**, *49*, 3557–3566. [CrossRef] [PubMed]
6. Tasca, F.; Farias, D.; Castro, C.; Acuna-Rougier, C.; Antiochia, R. Bilirubin Oxidase from Myrothecium verrucaria Physically Absorbed on Graphite Electrodes. Insights into the Alternative Resting Form and the Sources of Activity Loss. *PLoS ONE* **2015**, *10*, e0132181. [CrossRef]
7. Venegas, R.; Recio, F.J.; Riquelme, J.; Neira, K.; Marco, J.F.; Ponce, I.; Zagal, J.H.; Tasca, F. Biomimetic reduction of O_2 in an acid medium on iron phthalocyanines axially coordinated to pyridine anchored on carbon nanotubes. *J. Mater. Chem. A* **2017**, *5*, 12054–12059. [CrossRef]
8. Santoro, C.; Babanova, S.; Erable, B.; Schuler, A.; Atanassov, P. Bilirubin oxidase based enzymatic air-breathing cathode: Operation under pristine and contaminated conditions. *Bioelectrochemistry* **2016**, *108*, 1–7. [CrossRef]
9. Venegas, R.; Recio, F.J.; Zuniga, C.; Viera, M.; Oyarzun, M.-P.; Silva, N.; Neira, K.; Marco, J.F.; Zagal, J.H.; Tasca, F. Comparison of the catalytic activity for O2 reduction of Fe and Co MN4 adsorbed on graphite electrodes and on carbon nanotubes. *Phys. Chem. Chem. Phys.* **2017**, *19*, 20441–20450. [CrossRef]
10. Majumdar, S.; Lukk, T.; Solbiati, J.O.; Bauer, S.; Nair, S.K.; Cronan, J.E.; Gerlt, J.A. Roles of Small Laccases from Streptomyces in Lignin Degradation. *Biochemistry* **2014**, *53*, 4047–4058. [CrossRef]
11. Augustine, A.J.; Kragh, M.E.; Sarangi, R.; Fujii, S.; Liboiron, B.D.; Stoj, C.S.; Kosman, D.J.; Hodgson, K.O.; Hedman, B.; Solomon, E.I. Spectroscopic Studies of Perturbed T1 Cu Sites in the Multicopper Oxidases Saccharomyces cerevisiae Fet3p and Rhus vernicifera Laccase: Allosteric Coupling between the T1 and Trinuclear Cu Sites. *Biochemistry* **2008**, *47*, 2036–2045. [CrossRef]
12. Stone, J.R.; Yang, S. Hydrogen Peroxide: A Signaling Messenger. *Antioxid. Redox Signal.* **2006**, *8*, 243–270. [CrossRef]
13. Johnson, D.L.; Thompson, J.L.; Brinkmann, S.M.; Schuller, K.A.; Martin, L.L. Electrochemical Characterization of Purified Rhus vernicifera Laccase: Voltammetric Evidence for a Sequential Four-Electron Transfer. *Biochemistry* **2003**, *42*, 10229–10237. [CrossRef]
14. Filip, J.; Tkac, J. The pH dependence of the cathodic peak potential of the active sites in bilirubin oxidase. *Bioelectrochemistry* **2014**, *96*, 14–20. [CrossRef] [PubMed]
15. Solomon, E.I.; Sundaram, U.M.; Machonkin, T.E. Multicopper Oxidases and Oxygenases. *Chem. Rev.* **1996**, *96*, 2563–2606. [CrossRef] [PubMed]

16. Mano, N.; Edembe, L. Bilirubin oxidases in bioelectrochemistry: Features and recent findings. *Biosens. Bioelectron.* **2013**, *50*, 478–485. [CrossRef] [PubMed]
17. Cracknell, J.A.; Blanford, C.F. Developing the mechanism of dioxygen reduction catalyzed by multicopper oxidases using protein film electrochemistry. *Chem. Sci.* **2012**, *3*, 1567–1581. [CrossRef]
18. Murao, S.; Tanaka, N. A new enzyme "bilirubin oxidase" produced by Myrothecium verrucaria MT-1. *Agric. Biol. Chem.* **1981**, *45*, 2383–2384. [CrossRef]
19. Goldfinch, M.E.; Maguire, G.A. Investigation of the use of bilirubin oxidase to measure the apparent unbound bilirubin concentration in human plasma. *Ann. Clin. Biochem.* **1988**, *25*, 73–77. [CrossRef]
20. Tsujimura, S.; Fujita, M.; Tatsumi, H.; Kano, K.; Ikeda, T. Bioelectrocatalysis-based dihydrogen/dioxygen fuel cell operating at physiological pH. *Phys. Chem. Chem. Phys.* **2001**, *3*, 1331–1335. [CrossRef]
21. Palmore, G.T.R.; Kim, H.-H. Electro-enzymatic reduction of dioxygen to water in the cathode compartment of a biofuel cell. *J. Electroanal. Chem.* **1999**, *464*, 110–117. [CrossRef]
22. Mano, N.; Kim, H.-H.; Heller, A. On the Relationship between the Characteristics of Bilirubin Oxidases and O2 Cathodes Based on Their "Wiring". *J. Phys. Chem. B* **2002**, *106*, 8842–8848. [CrossRef]
23. Milton, R.D.; Giroud, F.; Thumser, A.E.; Minteer, S.D.; Slade, R.C.T. Bilirubin oxidase bioelectrocatalytic cathodes: The impact of hydrogen peroxide. *Chem. Commun. (Cambridge, UK)* **2014**, *50*, 94–96. [CrossRef] [PubMed]
24. Sakurai, T.; Kataoka, K. Basic and applied features of multicopper oxidases, CueO, bilirubin oxidase, and laccase. *Chem. Rec.* **2007**, *7*, 220–229. [CrossRef] [PubMed]
25. Solomon, E.I.; Augustine, A.J.; Yoon, J. O_2 Reduction to H_2O by the multicopper oxidases. *Dalton Trans.* **2008**, 3921–3932. [CrossRef] [PubMed]
26. Kjaergaard, C.H.; Durand, F.; Tasca, F.; Qayyum, M.F.; Kauffmann, B.; Gounel, S.; Suraniti, E.; Hodgson, B.; Hedman, K.O.; Mano, N.; et al. Spectroscopic and Crystallographic Characterization of "Alternative Resting" and "Resting Oxidized" Enzyme Forms of Bilirubin Oxidase: Implications for Activity and Electrochemical Behavior of Multicopper Oxidases. *J. Am. Chem. Soc.* **2012**, *134*, 5548–5551. [CrossRef] [PubMed]
27. Kjaergaard, C.H.; Jones, S.M.; Gounel, S.; Mano, N.; Solomon, E.I. Two-Electron Reduction versus One-Electron Oxidation of the Type 3 Pair in the Multicopper Oxidases. *J. Am. Chem. Soc.* **2015**, *137*, 8783–8794. [CrossRef] [PubMed]
28. Barton, S.C.; Gallaway, J.; Atanassov, P. Enzymatic biofuel cells for implantable and microscale devices. *Chem. Rev. (Washington, DC, USA)* **2004**, *104*, 4867–4886. [CrossRef]
29. Gallaway, J.W.; Calabrese Barton, S.A. Effect of redox polymer synthesis on the performance of a mediated laccase oxygen cathode. *J. Electroanal. Chem.* **2009**, *626*, 149–155. [CrossRef]
30. Szamocki, R.; Flexer, V.; Levin, L.; Forchiasin, F.; Calvo, E.J. Oxygen cathode based on a layer-by-layer self-assembled laccase and osmium redox mediator. *Electrochim. Acta* **2009**, *54*, 1970–1977. [CrossRef]
31. Grattieri, M.; Scodeller, P.; Adam, C.; Calvo, E.J. Non-competitive reversible inhibition of laccase by H2O2 in osmium mediated layer-by-layer multilayer O_2 biocathodes. *J. Electrochem. Soc.* **2015**, *162*, G82–G86. [CrossRef]
32. Scodeller, P.; Carballo, R.; Szamocki, R.; Levin, L.; Forchiassin, F.; Calvo, E.J. Layer-by-layer self-assembled osmium polymer-mediated laccase oxygen cathodes for biofuel cells: The role of hydrogen peroxide. *J. Am. Chem. Soc.* **2010**, *132*, 11132–11140. [CrossRef]
33. Ackermann, Y.; Guschin, D.A.; Eckhard, K.; Shleev, S.; Schuhmann, W. Design of a bioelectrocatalytic electrode interface for oxygen reduction in biofuel cells based on a specifically adapted Os-complex containing redox polymer with entrapped Trametes hirsuta laccase. *Electrochem. Commun.* **2010**, *12*, 640–643. [CrossRef]
34. Jenkins, P.A.; Boland, S.; Kavanagh, P.; Leech, D. Evaluation of performance and stability of biocatalytic redox films constructed with different copper oxygenases and osmium-based redox polymers. *Bioelectrochemistry* **2009**, *76*, 162–168. [CrossRef] [PubMed]
35. Lalaoui, N.; Reuillard, B.; Philouze, C.; Holzinger, M.; Cosnier, S.; Le Goff, A. Osmium (II) Complexes Bearing Chelating N-Heterocyclic Carbene and Pyrene-Modified Ligands: Surface Electrochemistry and Electron Transfer Mediation of Oxygen Reduction by Multicopper Enzymes. *Organometallics* **2016**, *35*, 2987–2992. [CrossRef]
36. Shin, H.; Cho, S.; Heller, A.; Kang, C. Stabilization of a Bilirubin Oxidase-Wiring Redox Polymer by Quaternization and Characteristics of the Resulting O_2 Cathode. *J. Electrochem. Soc.* **2009**, *156*, F87–F92. [CrossRef]

37. Shin, H.; Kang, C. Co-electrodeposition of bilirubin oxidase with redox polymer through ligand substitution for use as an oxygen reduction cathode. *Bull. Korean Chem. Soc.* **2010**, *31*, 3118–3122. [CrossRef]
38. Mano, N.; Kim, H.-H.; Zhang, Y.; Heller, A. An Oxygen Cathode Operating in a Physiological Solution. *J. Am. Chem. Soc.* **2002**, *124*, 6480–6486. [CrossRef] [PubMed]
39. Poeller, S.; Beyl, Y.; Vivekananthan, J.; Guschin, D.A.; Schuhmann, W. A new synthesis route for Os-complex modified redox polymers for potential biofuel cell applications. *Bioelectrochemistry* **2002**, *87*, 178–184. [CrossRef]
40. Wang, X.; Falk, M.; Ortiz, R.; Matsumura, H.; Bobacka, J.; Ludwig, R.; Bergelin, M.; Gorton, L.; Shleev, S. Mediatorless sugar/oxygen enzymatic fuel cells based on gold nanoparticle-modified electrodes. *Biosens. Bioelectron.* **2012**, *31*, 219–225. [CrossRef]
41. Salaj-Kosla, U.; Poller, S.; Schuhmann, W.; Shleev, S.; Magner, E. Direct electron transfer of Trametes hirsuta laccase adsorbed at unmodified nanoporous gold electrodes. *Bioelectrochemistry* **2013**, *91*, 15–20. [CrossRef]
42. Leger, C.; Jones, A.K.; Albracht, S.P.J.; Armstrong, F.A. Effect of a Dispersion of Interfacial Electron Transfer Rates on Steady State Catalytic Electron Transport in [NiFe]-hydrogenase and Other Enzymes. *J. Phys. Chem. B* **2002**, *106*, 13058–13063. [CrossRef]
43. Dos Santos, L.; Climent, V.; Blanford, C.F.; Armstrong, F.A. Mechanistic studies of the 'blue' Cu enzyme, bilirubin oxidase, as a highly efficient electrocatalyst for the oxygen reduction reaction. *Phys. Chem. Chem. Phys.* **2010**, *12*, 13962–13974. [CrossRef] [PubMed]
44. Reiss, R.; Ihssen, J.; Thony-Meyer, L. Bacillus pumilus laccase: A heat stable enzyme with a wide substrate spectrum. *BMC Biotechnol.* **2011**, *11*, 9. [CrossRef] [PubMed]
45. Mano, N.; de Poulpiquet, A. O_2 Reduction in Enzymatic Biofuel Cells. *Chem. Rev. (Washington, DC, USA)* **2018**, *118*, 2392–2468. [CrossRef] [PubMed]
46. Gentil, S.; Carriere, M.; Cosnier, S.; Gounel, S.; Mano, N.; Le Goff, A. Direct electrochemistry of bilirubin oxidase from Magnaporthe orizae on covalently-functionalized MWCNT for the design of high-performance oxygen-reducing biocathodes. *Chem. Eur. J.* **2018**, *24*, 8404–8408. [CrossRef] [PubMed]
47. De Poulpiquet, A.; Kjaergaard, C.H.; Rouhana, J.; Mazurenko, I.; Infossi, P.; Gounel, S.; Gadiou, R.; Giudici-Orticoni, M.T.; Solomon, E.I.; Mano, N.; et al. Mechanism of chloride inhibition of bilirubin oxidases and its dependence on potential and pH. *ACS Catal.* **2017**, *7*, 3916–3923. [CrossRef] [PubMed]
48. Han, X.; Zhao, M.; Lu, L.; Liu, Y. Purification, characterization and decolorization of bilirubin oxidase from Myrothecium verrucaria 3.2190. *Fungal Biol.* **2012**, *116*, 863–871. [CrossRef]
49. Zafar, M.N.; Tasca, F.; Boland, S.; Kujawa, M.; Patel, I.; Peterbauer, C.K.; Leech, D.; Gorton, L. Wiring of pyranose dehydrogenase with osmium polymers of different redox potentials. *Bioelectrochemistry* **2010**, *80*, 38–42. [CrossRef]
50. Mano, N. Features and applications of bilirubin oxidases. *Appl. Microbiol. Biotechnol.* **2012**, *96*, 301–307. [CrossRef]
51. De Poulpiquet, A.; Ciaccafava, A.; Gadiou, R.; Gounel, S.; Giudici-Orticoni, M.T.; Mano, N.; Lojou, E. Design of a H_2/O_2 biofuel cell based on thermostable enzymes. *Electrochem. Commun.* **2014**, *42*, 72–74. [CrossRef]
52. Chen, X.; Yin, L.; Lv, J.; Gross, A.J.; Le, M.; Gutierrez, N.G.; Li, Y.; Jeerapan, I.; Giroud, F.; Berezovska, A.; et al. Stretchable and Flexible Buckypaper-Based Lactate Biofuel Cell for Wearable Electronics. *Adv. Funct. Mater.* **2019**, *29*, 1905785. [CrossRef]
53. Kang, C.; Shin, H.; Heller, A. On the stability of the "wired" bilirubin oxidase oxygen cathode in serum. *Bioelectrochemistry* **2006**, *68*, 22–26. [CrossRef] [PubMed]
54. Milton, R.D.; Minteer, S.D. Investigating the reversible inhibition model of laccase by hydrogen peroxide for bioelectrocatalytic applications. *J. Electrochem. Soc.* **2014**, *161*, H3011–H3014. [CrossRef]
55. Di Bari, C.; Mano, N.; Shleev, S.; Pita, M.; De Lacey, A.L. Halides inhibition of multicopper oxidases studied by FTIR spectroelectrochemistry using azide as an active infrared probe. *JBIC J. Biol. Inorg. Chem.* **2017**, *22*, 1179–1186. [CrossRef] [PubMed]
56. Vaz-Dominguez, C.; Campuzano, S.; Ruediger, O.; Pita, M.; Gorbacheva, M.; Shleev, S.; Fernandez, V.M.; De Lacey, A.L. Laccase electrode for direct electrocatalytic reduction of O_2 to H_2O with high-operational stability and resistance to chloride inhibition. *Biosens. Bioelectron.* **2008**, *24*, 531–537. [CrossRef]
57. Tominaga, M.; Sasaki, A.; Togami, M. Bioelectrocatalytic oxygen reaction and chloride inhibition resistance of laccase immobilized on single-walled carbon nanotube and carbon paper electrodes. *Electrochemistry (Tokyo, Jpn.)* **2016**, *84*, 315–318. [CrossRef]

58. Enaud, E.; Trovaslet, M.; Naveau, F.; Decristoforo, A.; Bizet, S.; Vanhulle, S.; Jolivalt, C. Laccase chloride inhibition reduction by an anthraquinonic substrate. *Enzym. Microb. Technol.* **2011**, *49*, 517–525. [CrossRef]
59. Jensen, U.B.; Vagin, M.; Koroleva, O.; Sutherland, D.S.; Besenbacher, F.; Ferapontova, E.E. Activation of laccase bioelectrocatalysis of O_2 reduction to H_2O by carbon nanoparticles. *J. Electroanal. Chem.* **2012**, *667*, 11–18. [CrossRef]
60. Boland, S. Integrating Enzymes, Electron Transfer Mediators and Mesostructured Surfaces to Provide Bio-Electroresponsive Systems. Ph.D. Thesis, National University of Ireland, Galway, Ireland, 2008.
61. Zafar, M.N.; Tasca, F.; Gorton, L.; Patridge, E.V.; Ferry, J.G.; Noll, G. Tryptophan Repressor-Binding Proteins from Escherichia coli and Archaeoglobus fulgidus as New Catalysts for 1,4-Dihydronicotinamide Adenine Dinucleotide-Dependent Amperometric Biosensors and Biofuel Cells. *Anal. Chem.* **2009**, *81*, 4082–4088. [CrossRef]
62. Antiochia, R.; Tasca, F.; Mannina, L. Osmium-Polymer modified carbon nanotube paste electrode for detection of sucrose and fructose. *Mater. Sci. Appl.* **2013**, *4*, 15–22. [CrossRef]
63. Kurbanoglu, S.; Zafar, M.N.; Tasca, F.; Aslam, I.; Spadiut, O.; Leech, D.; Haltrich, D.; Gorton, L. Amperometric Flow Injection Analysis of Glucose and Galactose Based on Engineered Pyranose 2-Oxidases and Osmium Polymers for Biosensor Applications. *Electroanalysis* **2018**, *30*, 1496–1504. [CrossRef]
64. Heller, A. Electrical connection of enzyme redox centers to electrodes. *J. Phys. Chem.* **1992**, *96*, 3579–3587. [CrossRef]
65. Recio, F.J.; Canete, P.; Tasca, F.; Linares-Flores, C.; Zagal, J.H. Tuning the Fe (II)/(I) formal potential of the FeN4 catalysts adsorbed on graphite electrodes to the reversible potential of the reaction for maximum activity: Hydrazine oxidation. *Electrochem. Commun.* **2013**, *30*, 34–37. [CrossRef]
66. Tasca, F.; Recio, F.J.; Venegas, R.; Geraldo, D.A.; Sancy, M.; Zagal, J.H. Linear versus volcano correlations for the electrocatalytic oxidation of hydrazine on graphite electrodes modified with MN4 macrocyclic complexes. *Electrochim. Acta* **2014**, *140*, 314–319. [CrossRef]

© 2019 by the authors. Licensee MDPI, Basel, Switzerland. This article is an open access article distributed under the terms and conditions of the Creative Commons Attribution (CC BY) license (http://creativecommons.org/licenses/by/4.0/).